Micromagnetic Simulations with MumMax3

Vineet Tiwari

The future of Skyrmion based storage device requires a well built racetrack on which we can achieve efficient and controlled skyrmion motion. This paper models such a racetrack from scratch as micromagnetic simulations using Mumax3. Moreover, this paper shows that we can simultaneously move double skyrmion on the same nanotrack, with a current density of the order of $10^{11}\ A/m^2$.

1 Introduction

Since 1948, magnetic storage devices have been used in audio, video and data recording applications. In 1947, Williams Kilburn tube was introduced which was the first electronic Random Access Memory (RAM). It made use of electrically charged spots written on the cathode ray tube as bits. However, this memory technology did not long very last as it was not very reliable. In 1950s, a new magnetic core memory technology emerged in which data was stored in the arrays of magnetic rings. This technology lasted for almost two decades. However, in 1968, the introduction of Dynamic Random Access Memory (DRAM) based on semiconductor technology out-shined the ongoing magnetic core memories. These devices provided better scalability, mass manufacturing options and was compatible with the rest of the electronics in the then-emerging integrated chips. Since then, electronic storage devices has been in the spotlight and it took the magnetic devices almost half a century to be seriously considered again as a product in the market.

During the last decade, the interest in the research of magnet based storage devices has been revived. Scientists used the domain structure of Ferromagnets to make memory devices which are known as Domain wall memory which is a type of Racetrack memory. In these devices, the domain wall inside a ferromagnet are moved by applying spin torque current and the information can be read by sensing the magnetization direction of the domains. The drawback of this technology is the high current density required to move the domain walls, which eventually increases the temperature of the nanowires, and ultimately damage the device. However, the discovery of a topologically protected magnetic structure, the Magnetic Skyrmions, has opened a very new scope of designing the racetrack memory. Magnetic skyrmions consists of swirling spin textures whose stability is ensured by topological protection that can be theoretically described by an integer number known as the skyrmion number, formally defined by,

$$Q = \frac{1}{4\pi}\int d^2\vec{x}\ \vec{m}.\left(\frac{\partial\vec{m}}{\partial x}\times\frac{\partial\vec{m}}{\partial y}\right)$$

These magnetic structures are found in those system that break the inversion symmetry. With bulk Dzyaloshinskii-Moriya interaction (DMI), systems such as $MnSi$, $Fe_{1-x}Co_xSi$, Cu_2OSeO_3, has chiral crystal structure that supports vortex-like skyrmions. However, systems with interfacial DMI favors hedgehog-like skyrmions. Heavy metal/ultrathin ferromagnetic layers such as Fe/Ir, Ni/Co and $Ta/CoFeB/TaO_x$ are a few examples of such systems. Although the stabilization of skyrmions in a magnetic structure is ensured by DMI, it was recently shown that the frustrated exchange interactions, dipolar fields and curvature fields may also be responsible for nucleation of skyrmions in ferromagnets.

Due to their small size (order of 1 nm–100 nm), strong stability and their low current-driving motions (as low as $10^6 A/m^2$), magnetic skyrmions have strong potential for applications in logic computing, racetrack memory devices, and in general magnetic information. There are two type of skyrmions, Bloch-like skyrmions

in which magnetic moments rotate around tangential planes (normal to the radial direction) and Néel-like skyrmions in which the magnetic moments rotate in the radial planes. The difference in magnetization structure of the two types of skyrmion allowed researchers to encode data in binary, 0 or 1 bits to each of the Néel and Bloch skyrmions. This led to the study of skyrmion racetrack memory, in which skyrmion is moved by applying spin torque current, which helps in transfering data from one end of the racetrack to the other end. But, while moving in presence of current, the skyrmion also experience a sidewards drift which comes due to the Skyrmion Hall effect. This drift drives the skyrmion away from the center which leads to the annihilation of skyrmions at the edges at high operating current. However, there are ways to suppress this drift, one by tuning the ratio of the damping constant (α) and the non-adiabaticity constant (β or ξ). In this paper, we will try to model such a nanotrack in which skyrmions can easily move without getting annihilated. As less we need to tune the (α) to (β) ratio, as better and practical system we get.

2 Theoretical Background

2.1 What is Spintronics?

In solid-state devices, the study of the intrinsic spin of the electron and its associated magnetic moment is known as Spintronics or Spin electronics. The magnetic moment of electrons comes from the fact that when an electron with charge $-e$ revolves around the nucleus, its path acts as an Amperian loop. Thus, this rotating charge induces a magnetic dipole moment as shown in the figure below;

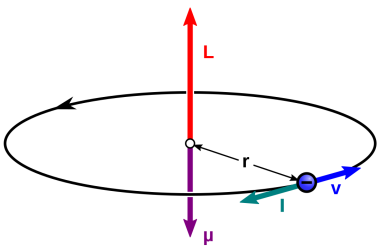

Figure 1: Schematic representation of the Electron's Magnetic moment (μ) and its Orbital Angular Momentum (L).[1]

Thus, due to this magnetic moment induced by the electron, each atom that has an unpaired electron in its valence shell has a net magnetic dipole moment, which we simply call spins. We represent the direction of this dipole moment by using an arrow, pointing either upwards or downwards depending upon the direction of rotation of electron around the nucleus.

Spintronics is one of the leading research interest branch of science. For the last few decades, researchers have found various future applications of spintronics which includes spin based transistors, Magnetoresistive Random Access Memory (MRAM) and Magnetic Racetrack memory etc.

2.2 Ferromagnets

In certain materials (usually transtion metals and their alloys), the spins are aligned parallel to each other in smaller regions of the materials. These smaller regions are called *Domains* (see Fig-2) and those materials that have one or more domains in it are known as *Ferromagnets*.

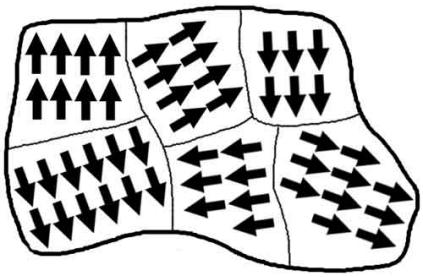

Figure 2: Figure showing the domains within a Ferromagnet.

The transition from one domain to the next domain is not a discrete switch of spins from one direction to another as shown in the figure above. The spins goes through a smooth transition from one domain to another domain. This smooth transition creates an interface that separates two neighbouring domain and thus are known as domain walls. Depending upon the rotation of spins within the walls, domain walls can further be categorized into two categories; Bloch walls and Néel walls. In the former category, the spins rotate within the plane of the wall, while in the later one the spins rotate in the plane perpendicular to the plane of the wall (see Fig-3).

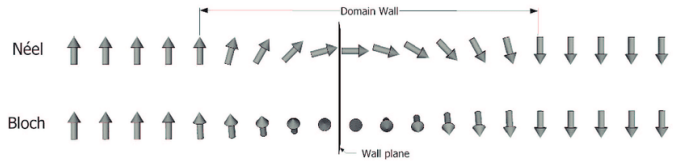

Figure 3: Schematic representation of a Néel wall and a Bloch wall. In both cases, the wall is the transition region between up and down magnetization, but they differ in the way the magnetization rotates. [9]

As already discussed, in presence of an external magnetic field, the domain walls break and all the spins get aligned in the direction of the applied field. Thus, as we keep applying the external field, we see that eventually all spins get aligned in the same direction and the magnet gets magnetized upto an upper value which we call as *Saturation magnetization*. However, in case of a ferromagnet, when we remove the external field, we see that there is still some magnetization left in the sample. This is known as the *retentivity* of the ferromagnet which is described as the residual magnetization of a ferromagnet when an external field is removed. In order to completely demagnetize the material, we need to apply another field in the opposite direction of the earlier field. Thus, we see at some negative field, the magnet gets completely demagnetized and this required negative field is known as the *Coercivity* of a ferromagnet. Moreover, if we keep applying the negative field, we will see that the magnet gets magnetized with the same amount but in the opposite direction. Interestingly, if we plot this applied field vs magnetization profile, we get the following loop (see Fig-4), which is also known as the Hysteresis loop.

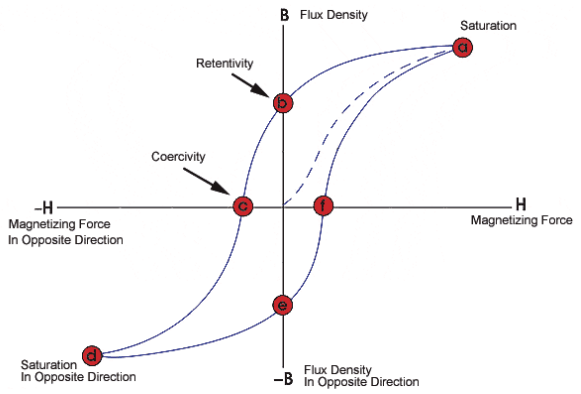

Figure 4: External applied field v/s Magnetization profile for a Ferromagnetic material. [12]

2.3 Various Energy terms in a Ferromagnet

There are various energy terms associated with the spin interactions of the electrons in the magnetic domain.

2.3.1 Heisenberg Exchange Energy

As its name reflects, the exchange interaction is the interaction between the neighbouring spins of a magnet. Generally, ferromagnets favour parallel alignment of neighbouring spins. In a magnetic solid, the exchange interaction acts between all pairs of neighbouring atoms, promoting the so called Heisenberg model. The Hamiltonian in this case is expanded to,

$$\mathcal{H} = -2 \cdot \sum_{i>j} \mathbf{S_1} \cdot \mathbf{S_2} \tag{1}$$

In eq(1) $i > j$ takes care for the over-counting of the spin pairs. The calculation of the exchange integral depends on the choice of electrons to be considered as well as the crystal environment such that a number of well studied exchange interactions can be defined

2.3.2 Magnetocrystalline Anisotropy Energy

The expression of the Heisenberg Hamiltonian is isotropic with respect to the crystal axis, as the the spin quantization axis does not have any spatial restrictions. This assumption does not suffer from loss of generality, but empirical evidence suggests that the magnetization does have a preferred direction of alignment, rather should depend on the crystalline environment. This is known as magneto-crystalline anisotropy. This mainly arises due to the correction to our previous Hamiltonian by including the effect such as spin-orbit coupling, dipole-dipole interaction as this breaks the rotational symmetry of the spin quantization axis. [6] The crystal anisotropy energy term must be a spatial function with the magnetization as an argument and as coefficients, some angular relation between the magnetization and the crystallographic axes. Thus we can write a power series in terms of the direction cosines, α_1, α_2, α_3 as,

$$E_{anis} = b_0 + \sum_{i=1,2,3} b_i \alpha_i + \sum_{i,j=1,2,3} b_i \alpha_i \alpha_j + \dots \tag{2}$$

where $(\alpha_1,\ \alpha_2,\ \alpha_3)$ = $(\sin\theta\cos\phi$,$\sin\theta\sin\phi,\ \cos\theta)$ with θ, ϕ the polar and azimuthal angles respectively. Moreover, experimental investigations show that the energy contribution of higher order terms in the expansion are compensated with thermal noise, such that mostly the first six order terms are included in the energy expression. As the energy cost associated with magneto-crystalline anisotropy is dependent on the crystal environment, it is expected that the formula takes a different expression for each crystal lattice. More accurately, it is the symmetry of the crystal environment that dictates the final form of the energy expression.

2.3.3 External Field Energy (Zeeman)

This term represents the energy cost of misalignment between an applied magnetic field and the magnetic moment of the sample. Consider a single spin with magnetic moment μ in a field H. The Hamiltonian in this case can be written as,

$$\mathcal{H} = \mu_0 \mu \cdot \mathbf{H} \tag{3}$$

In the continuum approximation, total *Zeeman Energy* for a system can be written as,

$$E_{Zeeman} = -\mu_0 M_s \int \mathbf{H} \cdot \mathbf{m} dV \tag{4}$$

2.3.4 Stray Field Energy (Demagnetization/ Magnetostatic)

In addition to the external applied field, the magnetization of the sample also creates a magnetic field inside the bulk, that opposes the field that created the magnetization in the first place. This secondary field also introduces an energy term. The demagnetizing (demag for short) field Hd can be thought to originate from the magnetic "*monopoles*"accumulating in the volume and on the surface of the sample.[7] Thus the following set of equations should make sense,

$$\nabla \cdot \mathbf{H}_d = \nabla \cdot \mathbf{M} \tag{5}$$

$$\nabla \times \mathbf{H}_d = 0 \tag{6}$$

From eq(5), and eq(6) we can conclude the following,

$$\mathbf{H}_d = -\nabla \phi \tag{7}$$

Where ϕ is some magnetic scalar potential. The calculation of the demagnetizing field and the respective energy is complex and generally calls for numerical evaluation, except in the most simple cases, such as an infinitely extended plate or an uniformly magnetized ellipsoid.

The stray field is mainly responsible for the formation of domains and domain walls inside a magnetic sample, with exceptions arising in special cases of shape, size and anisotropy. The same complexity argument that arises in the calculation of the demag-field is taken over to the calculation of domains and other magnetic textures. Numerical methods adapted for simulating magnetization dynamics consequently become an indispensable tool in the exploration of magnetic domains.

2.4 Magnetic Skyrmions

Magnetic skyrmions are small swirling topological defects in the magnetization texture, that are mostly induced by chiral interactions between atomic spins in non-centrosymmetric magnetic compounds or in films with broken inversion symmetry. These are pseudo-particles that can be created, moved and annihilated whose diameter ranges from a few to several hundreds of nanometers. Moreover, similar to the domain wall structure, skyrmions can also be divided into two categories depending upon the rotation of spins within the skyrmionic structure. Fig-5(a) shows the Bloch skyrmion in which the spins rotate in the tangential planes, that is, perpendicular to the radial directions, when moving from the core to the periphery. However, in a Néel skyrmion (see Fig-5(b)), the spins rotate in the radial planes from the core to the periphery.

The high stability and mobility makes skyrmion suitable for 'abacus'-type applications in information storage and logic technologies. Moreover, the two different structures as shown in the above figure can be used to write data in binary. The development of skyrmion-based spintronics holds promises for future applications in data storage and transfer.

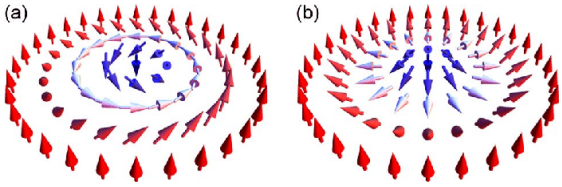

Figure 5: Bloch-type and Néel-type skyrmions. (a) In Bloch skyrmion, the spins rotate in the tangential planes, when moving from the core to the periphery. (b) In Néel skyrmion, the spins rotate in the radial planes from the core to the periphery. [9]

2.5 Racetrack Memory

The domain walls inside a ferromagnet can be moved by applying spin polarized current. So, if we stack a bunch of domains and store information with each domain, we can use this domain wall structure to store and transfer data. Moreover, the data can be read by sensing the magnetization direction of the domain. Hence, memories based on such a principle is known as a Domain wall memory. In racetrack memory, a ferromagnetic nanowire is formed on the silicon wafer, which can be configured horizontally or vertically (see Fig-6).

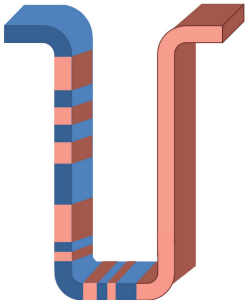

Figure 6: Domain walls in vertical configuration of nanowire. A bunch of such nanowires make a racetrack memory. [10]

These domain wall racetrack memories were seen as the potential candidate for magnet based data storage devices. But, the current density required to move a domain wall was very high (around $10^{12}\ A/m^2$), which leads to the heating of nanowire. Moreover, applying such a high value of current for a nanowire is very inefficient for practical purposes.

As we already discussed, skyrmions can be used to store data. Interestingly, it was observed that even the skyrmion moves in presence of an external magnetic field or spin polarized current. Thus, researchers tried out putting the skyrmion in a nanowire and moving with an external field which was carried out successfully. The current density required to move a skyrmion is much less than that of domain walls (from 10^6 to $10^{11}\ A/m^2$). Thus, the new concept of Skyrmion racetrack memory came into picture and became the potential candidate for spintronic data storage device. However, it was further observed that while moving in an electric current, skyrmions experience a drift which pushes it away from the center, which is known as the Skyrmion Hall effect. Due to SkHE, the skyrmions drift towards the edges and collides with them, which leads to the annihilation of skyrmions and thus the data gets deleted. Recently, antiferromagnetically exchange-coupled bilayer system has been reported for suppressing the SkHE. It can also be controlled by tuning the ratio of the damping constant (α) and the non-adiabaticity constant (β or ξ) of the material.

3 Materials and Methods

The system studied in this paper is an ultrathin Cobalt layer deposited on Platinum substrate which induces DMI. The material parameters for the same were; Saturation Magnetization $M_s = 5.8 \times 10^5\ A/m$, Exchange constant $A_{ex} = 1.5 \times 10^{-13}\ J/m$, DMI constant $D = 4 \times 10^{-3}\ mJ/m^2$, first order uni-axis Anisotropy constant $Ku_1 = 1 \times 10^6\ J/m^3$ in the z-direction and the damping constant α and the non-adiabaticity constant ξ was varied in the interval of 0.05 to 1.2 and 0.4 to 1 respectively. The cell size was kept at $2 \times 2 \times 2\ nm^3$.

The software used to simulate our system was Mumax3, which is a GPU-accelerated micromagnetic simulation program developed and maintained at the *DyNaMat* group at *Ghent University*. It calculates the space- and time-dependent magnetization dynamics in nano-sized to micro-sized ferromagnets using a finite-difference discretization. The governing equation of magnetization dynamics that our software solve is the Landau-Lifshitz-Gilbert (LLG) equation which has the mathematical form,

$$\frac{d\mathbf{m}}{dt} = -\gamma_{LL}(\mathbf{m} \times \mathbf{H_{eff}}) + \alpha_{LL}\mathbf{m} \times (\mathbf{m} \times \mathbf{H_{eff}}) \quad (8)$$

Where, $\gamma_{LL} = \gamma/(1+\alpha_G^2)$, and $\alpha_{LL} = \alpha_G\gamma/(1+\alpha_G^2)$, and where α_G is the Gilbert damping coefficient. Using this expression, it is possible to obtain the state of equilibrium of the magnetic system and implicitly the evolution of the magnetic texture under various time-dependent perturbations.

We started off by making a circular ring-like structure of outer diameter $200\ nm$ and inner diameter $50\ nm$ on a Co/Pt sample with Grid size $(256 \times 256 \times 2)$. We then induced a Néel skyrmion at the coordinates $(60, 0, 0)\ nm$ (see Fig-7) and injected a Spin-torque current of current density $(5\times10^{11}, 8\times10^{11}, 0)\ A/m^2$. The values for the damping constant α and non-adiabaticity constant ξ were 0.8 and 0.4 respectively.

Figure 7: Néel skyrmion on a ring-like structure to study the behaviour of skyrmion on a curved loop structure in the presence of an external spin-torque current. [11]

In this part, our main objective was to study the motion of skyrmion in a curved loop when an external current is applied, and how we can control that motion by tuning the values of α and ξ. The results of this part (which we will discuss in the next section) demanded us to extend our geometry into some different loop.

Thus, we modelled a new geometry which was in a shape of an infinity loop. Since, the size of this shape was more than twice the previous shape, our grid size in this part was kept at $(512, 256, 1)$. We then put a Néel skyrmion at the coordinates $(200, 130, 0)\ nm$ (see Fig-8.

Since, the main objective in this part was to check if we can move the skyrmion through the whole infinity-shaped path without getting annihilated at any point. We had two choices by which we could have controlled the direction of motion of the skyrmion,

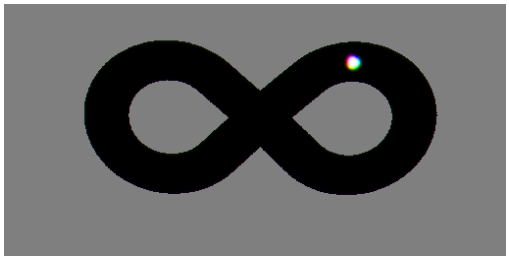

Figure 8: Néel skyrmion on a infinity loop structure to study the behaviour of skyrmion on a curved loop in the presence of an external spin-torque current. [11]

first by tuning the parameters like α and ξ at various region of the system, and second by changing the magnitude of current density injected in various region. For simulation purpose, the later option was more convenient in terms of the length of code required in this part, so we choose to vary the current at different regions of the system. The different values of the current in various parts can be found in ***APPENDIX***. As we will further discuss in the next section, we successfully moved the skyrmion in the loop. However, in the simulation, we had to change the current density very frequently near the leftmost and rightmost turning curved regions of the infinity shape, which makes the work very inefficient for practical purposes.

Fortunately, since our ultimate aim was to model a nanotrack, we thought of cutting out the end turning curved regions and applying a periodic boundary condition in the x-direction. This idea led me to my final geometry of the nanotrack that I was looking for, shown in Fig-9, and it also removed the most inefficient part of the geometry.

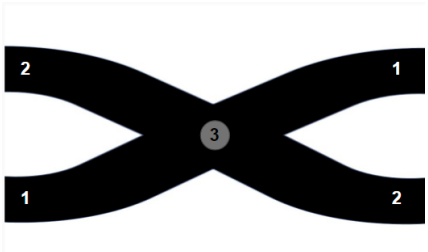

Figure 9: An infinitely long chain structure which is modelled as a nanotrack for transferring skyrmion that can ultimately be used in Skyrmion racetrack memory. [11]

The grid size in this part was kept as $(256,\ 180,\ 1)$ and as shown in Fig-9, the structure is divided into three regions in which he had different values of α and ξ.

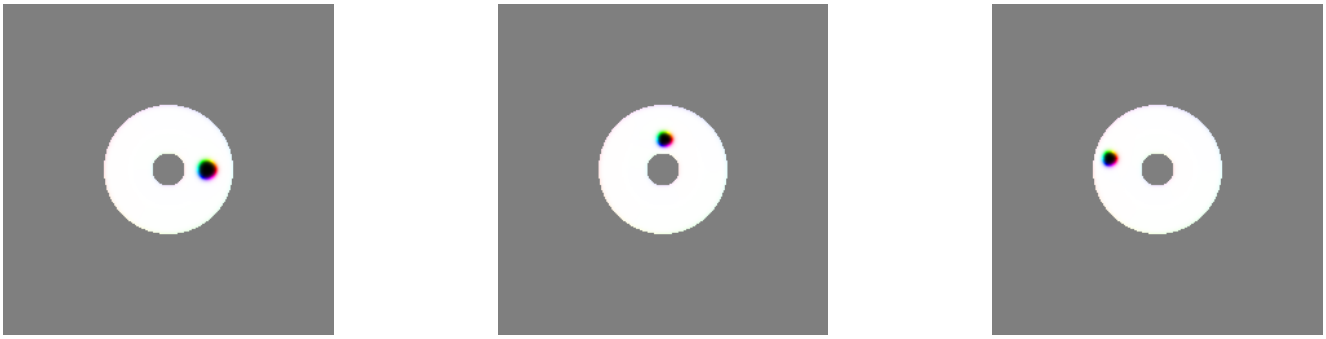

(a) (b) (c)

Figure 10: The position of skyrmion moving in the circular ring like structure. (a) Initial position of the skyrmion at zero current density. (b) Intermediate position of skyrmion in the ring. (c) Final position of skyrmion after which it stopped moving. [11]

Unlike the previous part, we injected a constant current, $j = (6 \times 10^{11}, -3.5 \times 10^{11}, 0)\ A/m^2$, throughout the system and changed the values of α and ξ. In region 1 and 3, the values were $\alpha = 0.05$ and $\xi = 1$, while in region 2 we had $\alpha = 0.5$ and $\xi = 0.6$. Region 3 in the system made sure that the skyrmion in the upper branch remains in the upper branch and same for the lower branch.

4 Results

In the first part, when we injected the current, we observed that the skyrmion moved halfway through the ring and then it stopped at one point (see Fig-10). After that, the skyrmion did not move at all which is clearly reflected in the velocity profile of the skyrmion (Fig-11)

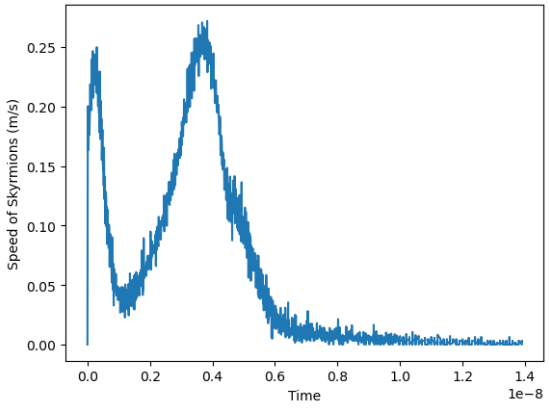

Figure 11: The Velocity profile of the skyrmion moving in the circular ring like structure. Here, we can clearly see that the skyrmion velocity gradually reaches to zero after 10 ns.

The most interesting observation was that the skyrmion did not move further and did not collide with the wall after 10 ns. It just sat there for the whole time, which just led us to the idea that in some sense it is waiting for a suitable path in tangential direction to move further. This logic might not sound very scientific but as we tangentially extended the path provided to the skyrmion, it actually moved. There could be a number of reasons why it stopped moving at that particular spot, but our vague logic of extending tangential path was certainly a solution that allowed the skyrmion to move further.

Thus, the extended shape that we got was an Infinity loop as shown in Fig-8. We induced the skyrmion on the left side of the shape and induced a current that helped it to move from the top right to the bottom left. Then, in order to move it from the bottom left to top left, we had to change the value of the current density twice. Then, we again changed the value of the current density to move the skyrmion from the top left to bottom right. Lastly, we had to again change the value of the current density twice to move the skyrmion from the bottom right to top right. And in this way, skyrmion moves in a complete loop without getting annihilated.

But, it is quite obvious that the procedure that we followed is very inefficient, but it is worth using as our main objective was to check if we can trap the skyrmion movement inside the loop, which we achieved. Moreover, the current density required to move the skyrmion in this system was of the order of $10^{12}\ A/m^2$, which is pretty high and inefficient. On contrary, this model really helped us understand that the skyrmion motion from the top section of one of the branch to the bottom section of the other branch is

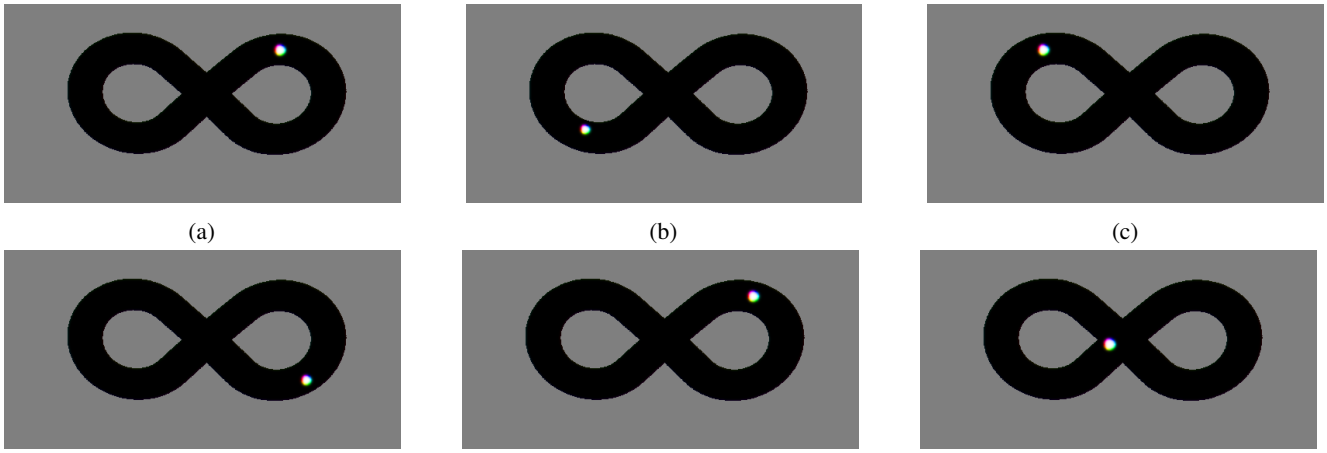

(a) (b) (c)

(d) (e) (f)

Figure 12: The positions of skyrmion moving in the infinity-shaped closed structure. (a) Initial position of the skyrmion at zero current density. (b) Skyrmion moved from the top left to the bottom right at $(2.5 \times 10^{12}, 0.1 \times 10^{12}, 0)\ A/m^2$. (c) Skyrmion moved from the bottom right to the top right at $(0.9 \times 10^{12}, -2.1 \times 10^{12}, 0)\ A/m^2$ and then $(2.5 \times 10^{12}, 0.1 \times 10^{12}, 0)\ A/m^2$. (d) Skyrmion moved from the top right to the bottom left at $(2 \times 10^{12}, 0.3 \times 10^{12}, 0)\ A/m^2$. (e) Skyrmion moved from the bottom left to the top left at $(0.9 \times 10^{12}, -2.1 \times 10^{12}, 0)\ A/m^2$ and then$(0.9 \times 10^{12}, -2.1 \times 10^{12}, 0)\ A/m^2$. (f) Skyrmion following the same trajectory as (a). [11]

governed by a constant set of parameters. We do not have to change any values in between these transitions, i.e. skyrmion going from Fig-12a to Fig-12b and from Fig-12c to Fig-12d. This idea helped us in building the final nanotrack in which skyrmion moved in an infinitely long track in a rather efficient manner.

2medskip

So, from the previous approach, we saw that the sharp curve turns were the most difficult region to move the skyrmion. So, the very first thought that comes into one's mind is to cut out that part, and we did exactly that. We removed the curvy turning ends on both sides and then applied periodic boundary conditions in the x-direction (see Fig-9). In this way, we were able to make a long nanotrack as a skyrmion, hence a path for information/data carrier. As already mentioned in the previous section, we divided our geometry into three regions with different values of α and β, which helped in a controlled motion of the skyrmion. Moreover, the current density that was required to move the skyrmion was of the order of 10^{11}, which is less than that is required in the previous part. The very first result that we got is shown in the figures below;

As expected, the skyrmion kept in the upper branch stayed in the upper branch. Once it arrived and crossed the left end of the upper branch, it re-entered from the right end due to the periodic boundary condition. Thus, if we visualise the upper branch with the periodic boundary condition, it appears as a long track on which the skyrmion can be moved to a very large distances which will help us in data transfer. We also tried putting a skyrmion in the lower branch and we saw that it also moved through the center and stayed in the lower branch of the system. Moreover, it also followed the periodic boundary condition and kept moving in the lower branch.

Lastly, as we saw that we can control the skyrmion motion in both the upper and lower branch, we thought of putting a skyrmion in both the branches simultaneously. This double skyrmion system is an extension to our previous system which will help us in transferring more data at the same time. The results are shown in Fig-14

So, from the sub-figures in Fig-14, we can clearly see that both the skyrmions move independently in their own assigned branch, and even in a long run, it is observed that the skyrmions never collide with each other at any point. This assures us that there is no risk of loosing data in this nanotrack. In the simulation video (attached in the appendix), we also observed that the skyrmion in the upper branch moves faster than the one in the lower branch, which is also evident from Fig-14. The possible reason behind this speed lag could be the difference in the values of α and ξ in various regions of

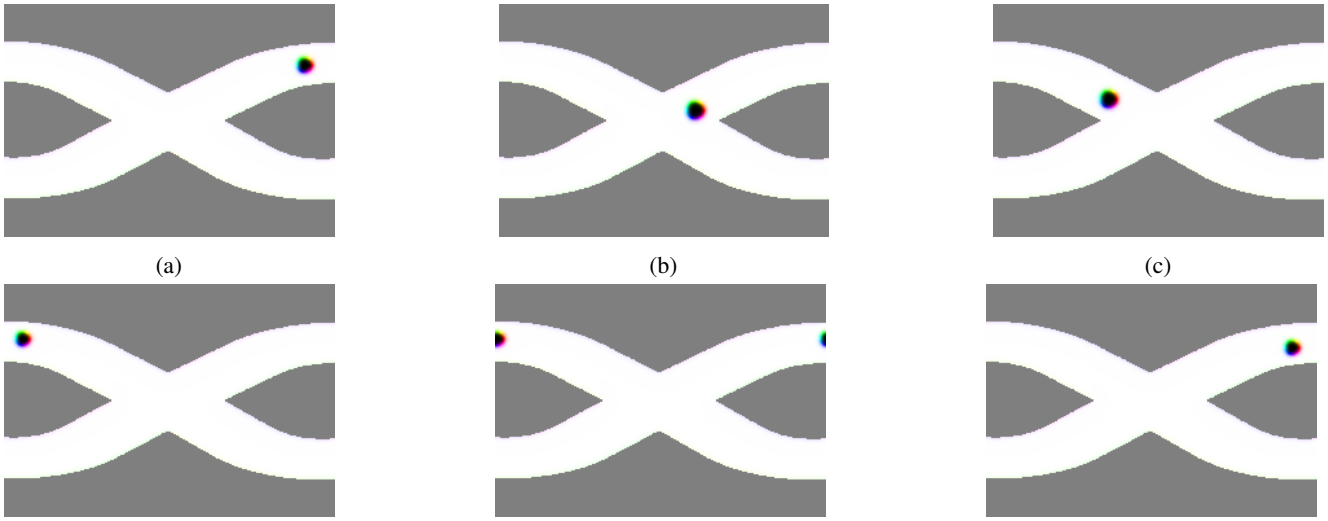

Figure 13: A single skyrmion placed on an infinitely long chain shaped nanotrack. (a) Initial position of the skyrmion. (b) Skyrmion reaching halfway to the center of the nanotrack. (c) Skyrmion crosses the center of the nanotrack and stays in the upper branch of the track. (d) Skyrmion almost reaching the leftmost boundary of the upper branch. (e) Skyrmion leaving the upper branch at one end and entering from the other end which shows the PBC. (f) Skyrmion successfully entered the upper branch from the right end and then it will repeat the same trajectory. [11]

the system. Say, if we ignore the effect of α and ξ for a second, we know for sure that the current will be the only external force that is driving the skyrmion. But, as soon as we increase α and ξ, we add extra factors that determine the direction of motion of skyrmions, and while doing so these factors also oppose or helps the effect of current on skyrmion. Therefore, a lot of times, while changing the trajectory of skyrmion in a desired direction, the change in α and ξ affects the speed of skyrmion. We were not able to find the exact difference between the speed of the two skyrmions. For this purpose, we need to separately analyze our

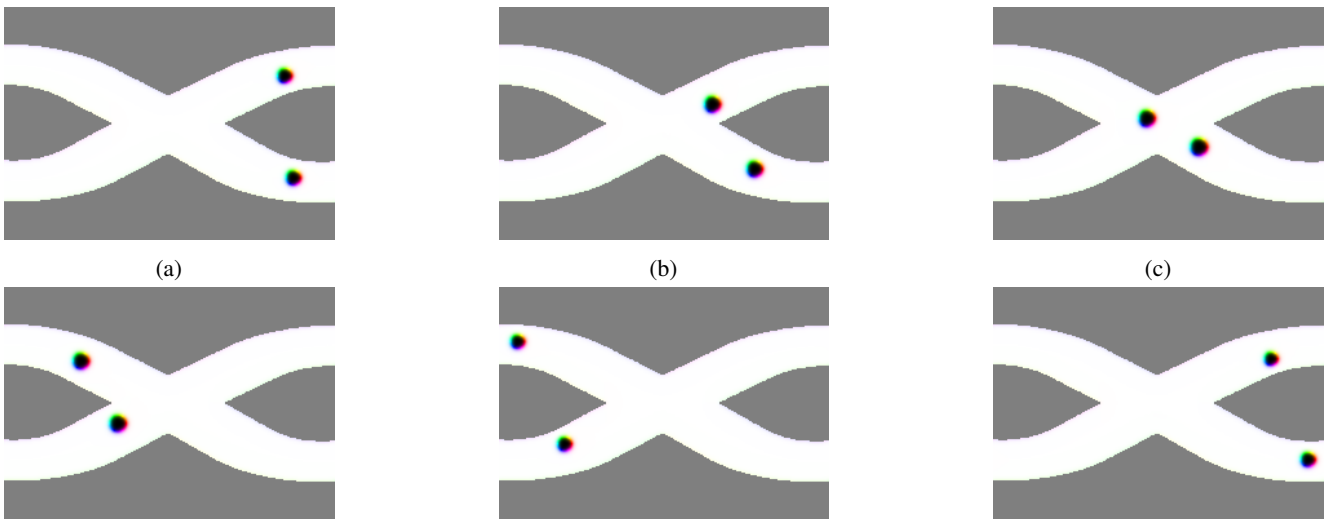

Figure 14: Double skyrmion placed on an infinitely long chain shaped nanotrack. (a) Initial position of the skyrmions in the upper and lower branch. (b) Skyrmions reaching halfway to the center of the nanotrack. (c) Skyrmions crosses the center of the nanotrack and stays in the upper branch of the track. (d) Skyrmions almost reaching the leftmost boundary of the upper branch. (e) Skyrmion leaving the upper branch at one end and entering from the other end which shows the PBC. (f) Skyrmion successfully entered the upper branch from the right end and then it will repeat the same trajectory. [11]

simulation videos, which is our future objective.

5 Conclusion and Prospects

In this paper, we studied the skyrmion motion in presence of spin-torque current in various systems. We started off by making a circular ring-like structure, in which we translated a skyrmion using current density of the order $10^{11}\ A/m^2$. The behaviour of the skyrmion in this system opened the scope of our new system, which was an Infinity loop in which we successfully moved the skyrmion. But, the current required to move the skyrmion at the curvy edges was of the order $10^{12}\ A/m^2$. So, we cut out the curvy edges and put a boundary condition in the x-direction, that helped us in making a long nanotrack. We successfully moved skyrmion in this nanotrack with the current density of the order $10^{11}\ A/m^2$, which is actually a very high amount of current for such nanoscale applications. So, one of our future goal is to reduce the current required to move the skyrmion, so that we can make more practically acceptable and efficient model of a nanotrack. Since, this paper was about the making of micromagnetic simulations using Mumax3, we haven't really analyzed anything from those simulations so far. So, our another future objective is to analyze the velocity profile of the single and double skyrmion structure.

6 Acknowledgement

I would like to acknowledge the constant support and guidance from Prof. Susmita Saha throughout the course of this ISM. I would extend my gratitude to Riya Mehta, Nitin Jha and Satwik Wats for their help in various part of this project.

References

[1] File:electron-orbital-magnetic-moment.svg (no date) Wikimedia Commons. Available at: https://commons.wikimedia.org/wiki/File:Electron-orbital-magnetic-moment.svg (Accessed: February 9, 2023).

[2] Henke, J. (2020) Louis Néel: Meester van het magnetisme, the Quantum Universe. Available at: https://www.quantumuniverse.nl/louis-neel-meester-van-het-magnetisme (Accessed: February 9, 2023).

[3] F. Williams, T. Kilburn, Nature 162 (4117) (1948) 487.

[4] F. Williams, T. Kilburn, G. Tootill, Proc. IEE 98 (61 Pt 2) (1951) 13–28.

[5] J.C. Slonczewski, J. Magn. Magn. Mater. 159 (1) (1996) L1–L7.

[6] Feilhauer, J., et al. "Controlled Motion of Skyrmions in a Magnetic Antidot Lattice." Physical Review B, vol. 102, no. 18, 2020, https://doi.org/10.1103/physrevb.102.184425.

[7] Tomasello, R., Martinez, E., Zivieri, R. et al. A strategy for the design of skyrmion racetrack memories. Sci Rep 4, 6784 (2014). https://doi.org/10.1038/srep06784

[8] Yuan, H., Wang, X. Erratum: Skyrmion Creation and Manipulation by Nano-Second Current Pulses. Sci Rep 6, 34898 (2016). https://doi.org/10.1038/srep34898

[9] Skyrmion-Electronics: An overview and outlook - IEEE XPLORE (no date). Available at: https://ieeexplore.ieee.org/abstract/document/7544451/ (Accessed: February 9, 2023).

[10] (2017). Spintronics based random access memory: A review. Materials Today, 20(9), 530-548. https://doi.org/10.1016/j.mattod.2017.07.007

[11] "The design and verification of mumax3", AIP Advances 4, 107133 (2014).

[12] B-H curve or hysteresis loop - GCW gandhinagar (no date). Available at: https://gcwgandhinagar.com/econtent/document/1588244806UPHTE-601%20Unit3.7%20JU_Hysteresis%20Curve.pdf (Accessed: February 9, 2023).

7 Appendix

Please find attached the simulation videos here (https://drive.google.com/drive/folders/1Jv6W1c4fVCRlD2ViY_XIWQvSbD7KY35R?usp=share_link)